Saturated Absorption Spectroscopy

Experiment SAS

University of Florida — Department of Physics PHY4803L — Advanced Physics Laboratory

With few adjustments for Quantum Optics course at Stockholm University

Overview

You will use a tunable diode laser to carry out spectroscopic studies of the rubidium atom. You will measure the Doppler-broadened absorption profiles of the D2 transitions at 780 nm and then use the technique of saturated absorption spectroscopy to improve the resolution beyond the Doppler limit and measure the nuclear hyperfine splittings, which are less than 1 ppm of the wavelength. A Fabry-Perot optical resonator is used to calibrate the frequency scale for the measurements.

Saturated absorption experiments cited in the 1981 Nobel prize in physics and related techniques have been used in laser cooling and trapping experiments cited in the 1997 Nobel prize as well as Bose-Einstein condensation experiments cited in the 2001 Nobel prize. Although the basic principles are straightforward, you will only be able to unleash the full power of saturated absorption spectroscopy by carefully attending to many details.

References

- 1. Daryl W. Preston Doppler-free saturated absorption: Laser spectroscopy, Amer. J. of Phys. **64**, 1432-1436 (1996).
- 2. K. B. MacAdam, A. Steinbach, and C. laser system with grating feedback, and a unit for high precision laser experiments.

- saturated absorption spectrometer for Cs and Rb, Amer. J. of Phys. **60**, 1098-1111 (1992).
- 3. John C. Slater, Quantum Theory of Atomic Structure, Vol. I, (McGraw-Hill, 1960)

Theory

The purpose of this section is to outline the basic features observed in saturated absorption spectroscopy and relate them to simple atomic and laser physics principles.

Laser interactions—two-level atom

We begin with the interactions between a laser field and a sample of stationary atoms having only two possible energy levels. Aspects of thermal motion and multilevel atoms will be treated subsequently.

The difference $\Delta E = E_1 - E_0$ between the excited state energy E_1 and the ground state energy E_0 is used with Planck's law to determine the photon frequency ν associated with transitions between the two states:

$$\Delta E = h\nu_0 \tag{1}$$

This energy-frequency proportionality is why energies are often given directly in frequency Wieman A narrow band tunable diode units. For example, MHz is a common energy There are three transition processes involving atoms and laser fields:

Stimulated absorption in which the atom starts in the ground state, absorbs a photon from the laser field, and then ends up in the excited state.

Stimulated emission in which the atom starts in the excited state, emits a photon with the same direction, frequency, and polarization as those in the laser field, and then ends up in the ground state.

Spontaneous emission in which the atom starts in the excited state, emits a photon in an arbitrary direction unrelated to the laser photons, and then ends up in the ground state.

Stimulated emission and absorption are associated with external electromagnetic fields such as from a laser or thermal (blackbody) radiation. We consider spontaneous emission first—a process characterized by a transition rate or probability per unit time for an atom in the excited state to decay to the ground state. This transition rate will be denoted γ and is about $3.6 \times 10^7/\mathrm{s}$ (or 36 MHz) for the rubidium levels studied here.

In the absence of an external field, any initial population of excited state atoms would decay exponentially to the ground state with a mean lifetime $\Delta t = 1/\gamma \approx 28$ ns. In the rest frame of the atom, spontaneous photons are emitted in all directions with an energy spectrum having a mean $E = h\nu_0$ and a full width at half maximum (FWHM) ΔE given by the Heisenberg uncertainty principle $\Delta E \Delta t = \hbar$ or $\Delta E = \gamma \hbar$. Expressed in frequency units, the FWHM is called the natural linewidth and given the symbol Γ . Thus

$$\Gamma = \frac{\gamma}{2\pi} \tag{2}$$

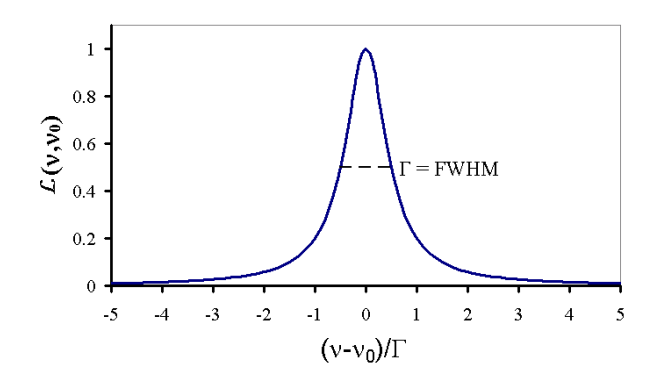


Figure 1: The Lorentzian line shape profile for resonance absorption.

For our rubidium levels, $\Delta E \approx 2.5 \times 10^{-8} \text{ eV}$ or $\Gamma \approx 6 \text{ MHz.}^{1}$

The stimulated emission and absorption processes are also described by a transition rate—a single rate giving the probability per unit time for a ground state atom to absorb a laser photon or for an excited state atom to emit a laser photon. The stimulated transition rate is proportional to the laser intensity I (SI units of W/m²) and is only significantly different from zero when the laser frequency ν is near the resonance frequency ν_0 . This transition rate will be denoted αI , where

$$\alpha = \alpha_0 \mathcal{L}(\nu, \nu_0) \tag{3}$$

and

$$\mathcal{L}(\nu,\nu_0) = \frac{1}{1 + 4(\nu - \nu_0)^2/\Gamma^2}$$
 (4)

gives the *Lorentzian* (or natural resonance) frequency dependence as shown in Fig. 1.

¹The natural linewidth Γ normally represents the sharpest observable energy distributions, but most attempts to measure it in gases are confounded by Doppler shifts associated with the random thermal motion of the atoms, which broaden the emission or absorption spectrum by an order of magnitude or more. Saturated absorption spectroscopy specifically overcomes the Doppler-broadening limit by providing for a two-photon interaction which only occurs for atoms with a lab frame velocity very near zero.

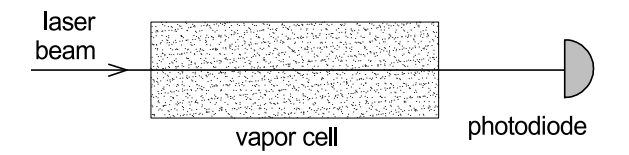


Figure 2: Basic arrangement for ordinary laser absorption spectroscopy.

 $\mathcal{L}(\nu, \nu_0)$ also describes the spectrum of radiation from spontaneous emission and the width Γ is the same for both cases. The maximum transition rate $\alpha_0 I$ occurs right on resonance $(\nu = \nu_0)$ and for the rubidium transitions studied here $\alpha_0 \approx 2 \times 10^6 \,\mathrm{m}^2/\mathrm{J}$.

The value of γ/α_0 defines a parameter of the atoms called the saturation intensity $I_{\rm sat}$

$$I_{\text{sat}} = \frac{\gamma}{\alpha_0} \tag{5}$$

and is about 1.6 mW/cm² for our rubidium transitions.² Its significance is that when the laser intensity is equal to the saturation intensity, excited state atoms are equally likely to decay by stimulated emission or by spontaneous emission.

Basic laser absorption spectroscopy

The basic arrangement for ordinary laser absorption (not saturated absorption) spectroscopy through a gaseous sample is shown in Fig. 2. A laser beam passes through the vapor cell and its intensity is measured by a photodiode detector as the laser frequency ν is scanned through the natural resonance frequency.

When a laser beam propagates through a gaseous sample, the two stimulated transition processes change the intensity of the laser

beam and affect the density of atoms (number per unit volume) in the ground and excited states. Moreover, Doppler shifts associated with the random thermal motion of the absorbing atoms must also be taken into account. There is an interplay among these effects which is critical to understanding saturated absorption spectroscopy. We begin with the basic equation describing how the laser intensity changes as it propagates through the sample and then continue with the effects of Doppler shifts and population changes.

Laser absorption

Because of stimulated emission and absorption, the laser intensity I(x) varies as it propagates from x to x + dx in the medium.

Exercise 1 Show that

$$I(x + dx) - I(x) = -h\nu\alpha I(x)(P_0 - P_1)n_0 dx$$
(6)

Hints: Multiply both sides by the laser beam cross sectional area A and use conservation of energy. Keeping in mind that I(x) is the laser beam intensity at some position x inside the vapor cell, explain what the left side would represent. With n_0 representing the overall density of atoms (number per unit volume) in the vapor cell, what does n_0Adx represent? P_0 and P_1 represent the probabilities that the atoms are in the ground and excited states, respectively, or the fraction of atoms in each state. They can be assumed to be given. What then is the rate at which atoms undergo stimulated absorption and stimulated emission? Finally, recall that $h\nu$ is the energy of each photon. So what would the right side represent?

Equation 6 leads to

$$\frac{dI}{dx} = -\kappa I \tag{7}$$

 $^{^{2}\}gamma$, Γ , α_{0} , $I_{\rm sat}$ vary somewhat among the various rubidium D2 transitions studied here. The values given are only representative.

where the absorption coefficient (fractional absorption per unit length)

$$\kappa = h\nu n_0 \alpha (P_0 - P_1) \tag{8}$$

The previous exercise demonstrates that the proportionality to $P_0 - P_1$ arises from the competition between stimulated emission and absorption and it is important to appreciate the consequences. If there are equal numbers of atoms in the ground and excited state $(P_0 - P_1 = 0)$, laser photons are as likely to be emitted by an atom in the excited state as they are to be absorbed by an atom in the ground state and there will be no attenuation of the incident beam. The attenuation maximizes when all atoms are in the ground state $(P_0 - P_1 = 1)$ because only upward transitions would be possible. And the attenuation can even reverse sign (become an amplification as it does in laser gain media) if there are more atoms in the excited state $(P_1 > P_0)$.

In the absence of a laser field, the ratio of the atomic populations in the two energy states will thermally equilibrate at the Boltzmann factor $P_1/P_0 = e^{-\Delta E/kT} = e^{-h\nu_0/kT}$. At room temperature, kT ($\approx 1/40$ eV) is much smaller than the $h\nu_0$ (≈ 1.6 eV) energy difference for the levels involved in this experiment and nearly all atoms will be in the ground state, i.e., $P_0 - P_1 = 1$. While you will see shortly how the presence of a strong laser field can significantly perturb these thermal equilibrium probabilities, for now we will only treat the case where the laser field is weak enough that $P_0 - P_1 = 1$ remains a good approximation throughout the absorption cell.

Doppler shifts

Atoms in a vapor cell move randomly in all directions with each component of velocity having a distribution of values. Only the component of velocity parallel to the laser beam

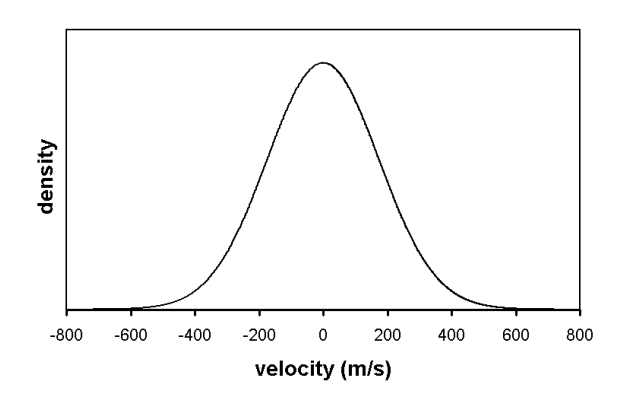


Figure 3: Maxwell-Boltzmann velocity distribution. The density of atoms vs. their velocity component in one direction for room temperature rubidium atoms.

direction will be important when taking into account Doppler shifts and it is this component we refer to with the symbol v. The density of atoms dn in the velocity group between v and v+dv is given by the Boltzmann velocity distribution:

$$dn = n_0 \sqrt{\frac{m}{2\pi kT}} e^{-mv^2/2kT} dv \tag{9}$$

With a standard deviation (proportional to the width of the distribution) given by:

$$\sigma_v = \sqrt{kT/m} \tag{10}$$

this is just a standard Gaussian distribution

$$dn = n_0 \frac{1}{\sqrt{2\pi} \sigma_v} e^{-v^2/2\sigma_v^2} dv$$
 (11)

with a mean of zero—indicating the atoms are equally likely to be going in either direction. It is properly normalized so that the integral over all velocities $(-\infty \to \infty)$ is n_0 , the overall atom density. Note that the distribution's variance σ_v^2 increases linearly with temperature and decreases inversely with atomic mass.

Exercise 2 Determine the width parameter σ_v of the Maxwell-Boltzmann distribution for room temperature rubidium atoms and compare with the plot of Fig. 3.

Atoms moving with a velocity v see the laser beam Doppler shifted by the amount v(v/c). We will take an equivalent, alternate view that atoms moving with a velocity v have a Doppler shifted resonance frequency

$$\nu_0' = \nu_0 \left(1 + \frac{v}{c} \right) \tag{12}$$

in the lab frame. The sign has been chosen to be correct for a laser beam propagating in the positive direction so that the resonance frequency is blue shifted to higher frequencies if v is positive and red shifted if v is negative.

The absorption coefficient $d\kappa$ from a velocity group dn at a laser frequency ν is then obtained from Eq. 8 by substituting dn for n_0 (keeping in mind its dependence on v through Eq. 9) and by adjusting the Lorentzian dependence of α so that it is centered on the Doppler shifted resonance frequency ν'_0 (keeping in mind its dependence on v through Eq. 12).

$$d\kappa = h\nu\alpha_0(P_0 - P_1)\mathcal{L}(\nu, \nu_0')dn \tag{13}$$

The absorption coefficient from all atoms is then found by integrating over all velocity groups. We treat the weak-laser case first setting $P_0 - P_1 = 1$ so that

$$d\kappa = n_0 h \nu \alpha_0 \sqrt{\frac{m}{2\pi kT}} \mathcal{L}(\nu, \nu_0') e^{-mv^2/2kT} dv$$
(14)

Exercise 3 (a) Show that the Lorentzian function $\mathcal{L}(\nu,\nu'_0)$ at a particular ν is significantly different from zero only for atoms with velocities within a very narrow range around

$$v_{probe} = c(\nu/\nu_0 - 1) \tag{15}$$

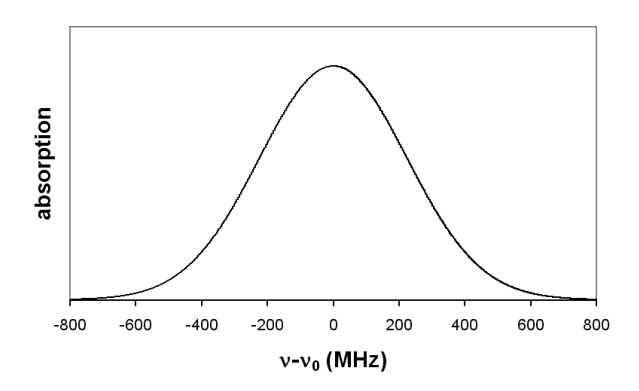


Figure 4: Doppler profile. The absorption coefficient vs. the laser frequency offset from resonance has a Gaussian lineshape.

(b) Determine the rough size of this range assuming $\Gamma = 6$ MHz. ($\nu_0 = c/\lambda$ where $\lambda = 780$ nm.) (c) Show that over this range, $e^{-mv^2/2kT}$ remains relatively constant, i.e., compare the range with σ_v (Eq. 10). Consequently, the integral of Eq. 14 can be accurately determined as the integral of the Lorentzian times the value of the exponential at $v = v_{probe}$. The integration of the Lorentzian $\int \mathcal{L}(\nu, \nu'_0) dv$ is easier to look up after using Eq. 12 to convert $dv = (c/\nu_0) d\nu'_0$. (d) Show that integrating the absorption coefficient $\int d\kappa$ over velocity (from $-\infty$ to ∞) then gives a Gaussian dependence on ν centered around the resonance frequency ν_0

$$\kappa = \kappa_0 e^{-(\nu - \nu_0)^2 / 2\sigma_\nu^2} \tag{16}$$

with the width parameter given by

$$\sigma_{\nu} = \nu_0 \sqrt{\frac{kT}{mc^2}} \tag{17}$$

and

$$\kappa_0 = n_0 h \nu \alpha_0 \sqrt{\frac{m}{2\pi k T}} \frac{c}{\nu_0} \frac{\pi \Gamma}{2}$$
 (18)

(e) Evaluate the Doppler-broadened width parameter σ_{ν} for room temperature rubidium atoms and compare your results with the profile illustrated in Fig. 4.

Populations

Now we would like to take into account the changes to the ground and excited state populations arising from a laser beam propagating through the cell. The rate equations for the ground and excited state probabilities or fractions become:

$$\frac{dP_0}{dt} = \gamma P_1 - \alpha I(P_0 - P_1)$$

$$\frac{dP_1}{dt} = -\gamma P_1 + \alpha I(P_0 - P_1) \qquad (19)$$

where the first term on the right in each equation arises from spontaneous emission and the second term arises from stimulated absorption and emission.

Exercise 4 (a) Show that steady state conditions (i.e., where $dP_0/dt = dP_1/dt = 0$) lead to probabilities satisfying

$$P_0 - P_1 = \frac{1}{1 + 2\alpha I/\gamma} \tag{20}$$

Hint: You will also need to use $P_0 + P_1 = 1$. (b) Show that when this result is used in Eq. 8 (for stationary atoms) and the frequency dependence of α as given by Eqs. 3-4 is also included, the absorption coefficient κ again takes the form of a Lorentzian

$$\kappa = \frac{h\nu n_0 \alpha_0}{1 + 2I/I_{sat}} \mathcal{L}'(\nu, \nu_0) \tag{21}$$

where \mathcal{L}' is a standard Lorentzian

$$\mathcal{L}'(\nu,\nu_0) = \frac{1}{1 + 4(\nu - \nu_0)^2/\Gamma'^2}$$
 (22)

with a power-broadened width parameter

$$\Gamma' = \Gamma \sqrt{1 + 2I/I_{sat}} \tag{23}$$

The approach to the steady state probabilities is exponential with a time constant around $[\gamma+2\alpha I]^{-1}$, which is less than 28 ns for our rubidium transitions. Thus as atoms, mostly in the ground state, wander into the laser beam at thermal velocities, they would only travel a few microns before reaching equilibrium probabilities.

C.Q. 1 Take into account velocity groups and their corresponding Doppler shifts for the case $P_0 - P_1 \neq 1$. The calculation is performed as in Exercise 3. Show that the result after integrating over all velocity groups is:

$$\kappa = \kappa_0' e^{-(\nu - \nu_0)^2 / 2\sigma_\nu^2} \tag{24}$$

where the width parameter, σ_{ν} is the same as before (Eq. 17), but compared to the weak-field absorption coefficient (Eq. 18), the strong-field coefficient decreases to

$$\kappa_0' = \frac{\kappa_0}{\sqrt{1 + 2I/I_{sat}}} \tag{25}$$

Laser absorption through a cell

In the weak-field case κ at any frequency is given by Eq. 16 (with Eq. 18) and is independent of the laser intensity. In this case, Eq. 7 is satisfied by Beer's law which says that the intensity decays exponentially with distance traveled through the sample.

$$I(x) = I_0 e^{-\kappa x} \tag{26}$$

In the general case, κ is given by Eq. 24 (with Eq. 25) and at any frequency is proportional to $1/\sqrt{1+2I/I_{\rm sat}}$. The general solution to Eq. 7 for how the laser intensity varies with the distance x into the cell is then rather more complicated than Beer's law and is given in an appendix that can be found on the lab web site. However, the strong-field $I >> I_{\rm sat}$ behavior is easily determined by neglecting the 1 compared to $I/I_{\rm sat}$ so that Eq. 7 becomes

$$\frac{dI}{dx} = -k\sqrt{I} \tag{27}$$

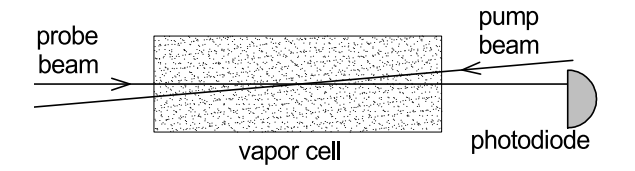


Figure 5: Basic arrangement for saturated absorption spectroscopy.

where

$$k = \kappa_0 \sqrt{I_{\text{sat}}/2} e^{-(\nu - \nu_0)^2/2\sigma_\nu^2}$$
 (28)

Saturated absorption—simple model

Up to now, we have considered only a single laser beam propagating through the cell. Now we would like to understand what happens when a second laser propagates through the cell in the opposite direction. This is the basic arrangement for saturated absorption spectroscopy shown in Fig. 5. The laser beam traveling to the right—the one we have been considering up to now and whose absorption is measured—is now called the *probe* beam. The second overlapping laser beam propagating in the opposite direction is called the pump beam. Both beams will be from the same laser and so they will have the same frequency, even as that frequency is scanned through the resonance.

With only a single weak laser propagating through the sample, $P_0 - P = 1$ would be a good approximation throughout the cell. With the two beams propagating through the cell, the probe beam will still be kept weak—weak enough to neglect its affect on the populations. However, the pump beam will be made strong—strong enough to significantly affect the populations and thus change the measured absorption of the probe beam. To understand how this comes about, we will again have to consider Doppler shifts.

As mentioned, the stimulated emission and absorption rates are nonzero only when the laser is near the resonance frequency. Thus, we will obtain P_0-P_1 from Eq. 20 by giving α a Lorentzian dependence on the Doppler shifted resonance frequency:

$$\alpha = \alpha_0 \mathcal{L}(\nu, \nu_0'') \tag{29}$$

with the important feature that for the pump beam, the resonance frequency for atoms moving with a velocity v is

$$\nu_0'' = \nu_0 \left(1 - \frac{v}{c} \right) \tag{30}$$

This frequency is Doppler shifted in the direction opposite that of the probe beam because the pump beam propagates through the vapor cell in the negative direction. That is, the resonant frequency for an atom moving with a signed velocity v is $\nu_0(1+v/c)$ for the probe beam and $\nu_0(1-v/c)$ for the pump beam.

Exercise 5 (a) Plot Eq. 20 versus the detuning parameter

$$\delta = \nu - \nu_0'' \tag{31}$$

for values of I/I_{sat} from 0.1 to 1000. (Use $\Gamma = 6$ MHz.) (b) Use your graphs to determine how the FWHM of the dips in $P_0 - P_1$ change with laser power.

Exercise 5 should have demonstrated that for large detunings $(\delta \gg \Gamma)$, $P_0 - P_1 = 1$ implying that in this case the atoms are in the ground state—the same as when there is no pump beam. On resonance, i.e., at $\delta = 0$, $P_0 - P_1 = 1/(1 + 2I/I_{\rm sat})$, which approaches zero for large values of I. This implies that atoms in resonance with a strong pump beam will have equal populations in the ground and excited states $(P_0 - P_1 = 0)$. That is, a strong,

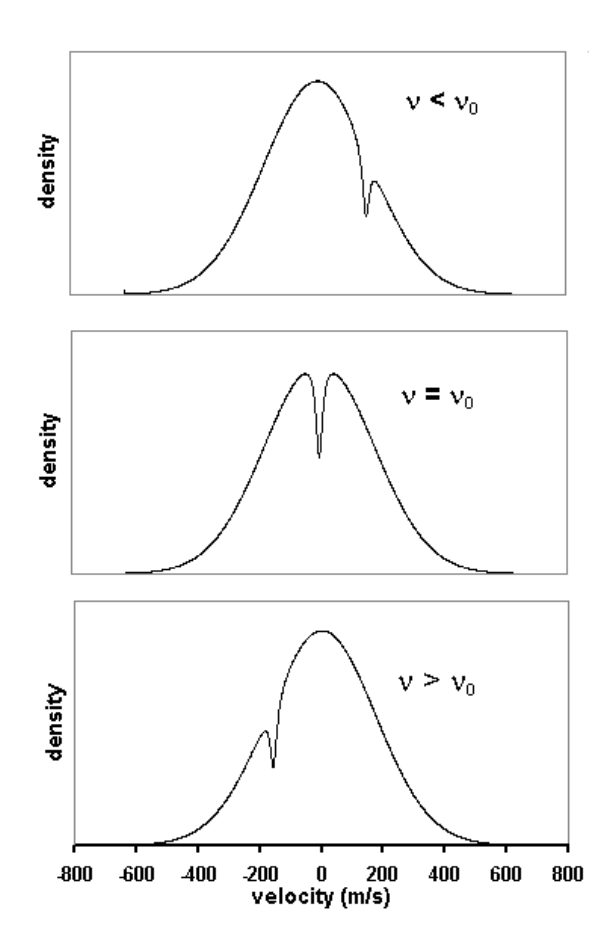


Figure 6: Hole burning by the pump beam. The density of ground state atoms is plotted vs. their velocity and becomes depleted near the velocity that Doppler shifts the laser frequency into resonance with ν_0 .

resonant laser field causes such rapid transitions in both directions that the two populations equilibrate. The laser is said to "saturate" the transition, which is the origin of the name of the technique.

According to Eq. 30, the resonance condition ($\delta = 0$) translates to $v = v_{\text{pump}}$ where

$$v_{\text{pump}} = c(1 - \nu/\nu_0) \tag{32}$$

Consequently, for any frequency ν within the Doppler profile, only atoms near this velocity will be at zero detuning and will have val-

ues of $P_0 - P_1$ perturbed from the "pump off" value of unity. Of course, whether there are a significant number of atoms in either level near $v = v_{\text{pump}}$ depends on the width of the Boltzmann velocity distribution and the relative values of ν and ν_0 . But if v_{pump} is within the distribution, the atoms near that velocity will have perturbed populations.

The density of atoms in the ground state $dn_1 = P_1 dn$ plotted as a function of v will follow the Maxwell-Boltzmann distribution except very near $v = v_{\text{pump}}$ where it will drop off significantly as atoms are promoted to the excited state. This is called "hole burning" as there is a hole (a decrease) in the density of atoms in the ground state near $v = v_{\text{pump}}$ (and a corresponding increase in the density of atoms in the excited state) as demonstrated in Fig. 6.

How does hole burning affect the probe beam absorption? In Exercise 3 you learned that the absorption at any frequency ν arises only from those atoms moving with velocities near $v_{\text{probe}} = c(\nu/\nu_0 - 1)$. Also recall, the probe beam absorption is proportional to $P_0 - P_1$, which we have just seen remains constant (≈ 1) except for atoms having nearly the exact opposite velocities near $v_{\text{pump}} = c(1 - \nu/\nu_0)$. Therefore, when the laser frequency is far from the natural resonance $(|\nu - \nu_0| \gg \Gamma)$, the probe absorption arises from atoms moving with a particular velocity in one direction while the pump beam is burning a hole for a completely different set of atoms with the opposite velocity. In this case, the presence of the pump beam will not affect the probe beam absorption which would follow the standard Doppler-broadened profile.

Only when the laser frequency is very near the resonance frequency ($\nu = \nu_0$, $v_{\text{probe}} = v_{\text{pump}} = 0$) will the pump beam burn a hole for atoms with velocities near zero which would then be the same atoms involved with the

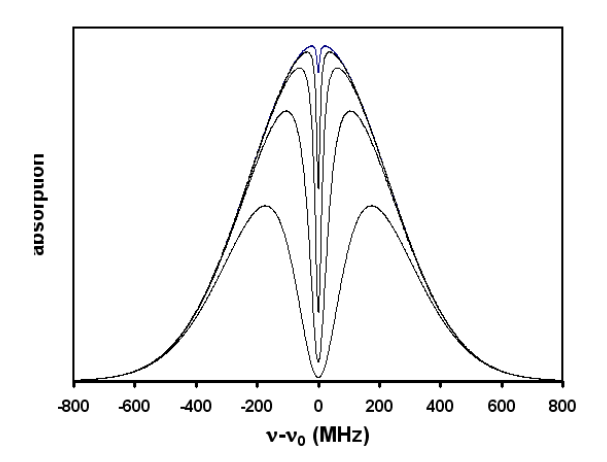


Figure 7: Absorption coefficient vs. the laser frequency offset from resonance for a two-level atom at values of $I/I_{\rm sat}=0.1,1,10,100,1000$ (from smallest dip to largest). It shows a Gaussian profile with the saturated absorption dip at $\nu=\nu_0$.

probe beam absorption at this frequency. The absorption coefficient would be obtained by taking P_1-P_0 as given by Eq. 20 (with Eqs. 29 and 30) to be a function of the laser frequency ν and the velocity v, using it in Eq. 13 (with Eqs. 9 and 12), and then integrating over velocity. The result is a Doppler-broadened profile with what's called a saturated absorption dip (or Lamb dip) right at $\nu = \nu_0$. Numerical integration was used to create the profiles shown in Fig. 7 for several values of $I/I_{\rm sat}$.

Multilevel effects

Real atoms have multiple upper and lower energy levels which add complexities to the simple two-level model presented so far. For this experiment, transitions between two lower levels and four upper levels can all be reached with our laser and add features called crossover resonances and a process called optical pumping. Crossover resonance are addi-

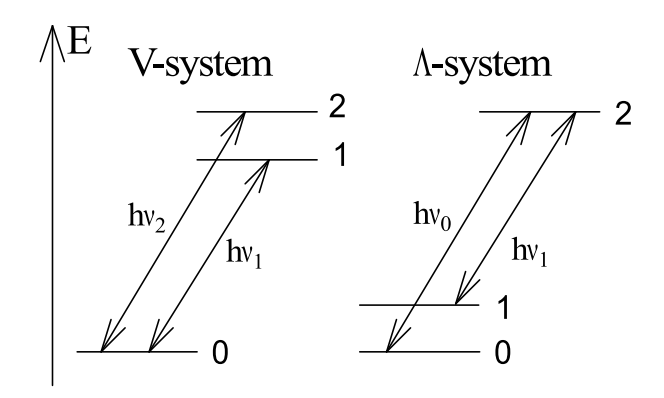


Figure 8: Energy levels for two possible threelevel systems. The V-configuration with two upper levels and the) Λ -system with two lower levels.

tional narrow absorption dips arising because several upper or lower levels are close enough in energy that their Doppler-broadened profiles overlap. Optical pumping occurs when the excited level can spontaneously decay to more than one lower level. It can significantly deplete certain ground state populations further enhancing or weakening the saturated absorption dips.

The basics of crossover resonances can be understood within the three-level atom in either the Λ - or V-configurations shown in Fig. 8 where the arrows represent allowed spontaneous and stimulated transitions. In this experiment, crossover resonances arise from multiple upper levels and so we will illustrate with the V-system. Having two excited energy levels 1 and 2, the resonance frequencies to the ground state 0 are ν_1 and ν_2 , which are assumed to be spaced less than a Doppler width apart.

Without the pump beam, each excited state would absorb with a Doppler-broadened profile and the net absorption would be the sum of two Gaussian profiles, one centered at ν_1 and

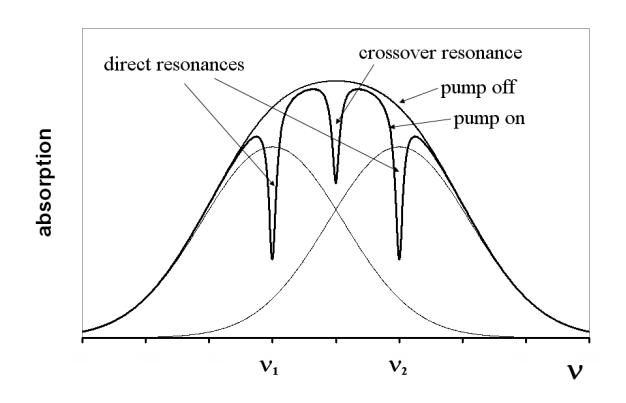


Figure 9: Absorption coefficient vs. the laser frequency for a V-type three-level atom. The three Bell shaped curves are with the pump off and give the Doppler-broadened absorption from the individual resonances at ν_1 and ν_2 and their sum. The pump on curve shows normal saturated absorption dips at $\nu = \nu_1$ and $\nu = \nu_2$ and a crossover resonance midway between.

one centered at ν_2 . If the separation $|\nu_1 - \nu_2|$ is small compared to the Doppler width, they would appear as a single broadened absorption profile.

When the pump beam is turned on, two holes are burned in the ground state velocity distribution at velocities that put the atoms in resonance with ν_1 and ν_2 . These two velocities would depend on the laser frequency ν . For example, at $\nu = \nu_1$, the probe absorption involving upper state 1 is from $v \approx 0$ atoms while the probe absorption involving the higher-energy state 2 arises from some nonzero, negativevelocity atoms. At this frequency, the pump beam burns one hole in the ground state for $v \approx 0$ atoms due to upper state 1 and another hole for some nonzero, positive-velocity atoms due to upper state 2. As with the two-level system, the hole at $v \approx 0$ leads to a decreased absorption to upper state 1 and produces a saturated absorption dip at $\nu = \nu_1$. A similar argument predicts a saturated absorption dip at $\nu = \nu_2$. Thus at $\nu = \nu_1$ and at $\nu = \nu_2$ there will be saturated absorption dips similar to those occurring in two-level atoms.

A third dip, the crossover resonance, arises at a frequency midway between—at $\nu_{12} = (\nu_1 + \nu_2)/2$. All three dips are illustrated in Fig. 9 assuming $I/I_{\rm sat} = 10$ and assuming that the excited levels have the same spontaneous transitions rate γ and the same stimulated rate constant α_0 .

At the crossover frequency, the pump and probe beams are resonant with the same two opposite velocity groups: $v \approx \pm c (\nu_2 - \nu_1)/2\nu_{12}$. Atoms at one of these two velocities will be resonant with one excited state and atoms at the opposite velocity will be resonant with the other excited state. The pump beam burns a hole in the ground state populations at both velocities and these holes affect the absorption of the probe beam, which is simultaneously also arising from atoms with these two velocities.

C.Q. 2 Explain why the crossover resonance dip disappears as the laser frequency changes by a few linewidths from the mid-frequency where the dip occurs. Remember, in this region each beam will still be interacting with two velocity groups: one group for one excited state and another for the other excited state. For example, consider the case where the laser goes above the mid-frequency by a small amount. How would the velocities change for the two groups of atoms involved in probe beam absorption? How would the velocities change for the two groups of atoms involved in pump beam absorption?

Optical pumping in rubidium occurs where one excited level can decay to two different lower levels. It can be modeled in terms of the Λ -type three-level atom, where the two lower

levels are separated in energy by much more **Energy levels in rubidium** than a Doppler width.

Assume the laser beam is resonant with atoms in only one of the lower levels, but atoms in the excited level spontaneously decay to either lower level more or less equally. Then, each time an atom in the "resonant" lower level is promoted by the laser to the excited level, some fraction of the time it will decay to the "non-resonant" lower level. Once in the non-resonant lower level, the atom no longer interacts with the laser field. It becomes "shelved" and unable to contribute to the absorption. Analysis of the level populations then requires a model where atoms outside the laser beam interaction volume randomly diffuse back into it thereby replenishing the resonant lower level populations. Depending on the laser intensity and beam geometry, the lower level populations can be significantly altered by optical pumping.

As with the population variations arising from stimulated emission and absorption, optical pumping also depends on the laser frequency and atom velocities. Optical pumping due to the pump beam can drastically deplete resonant ground state atoms and can significantly increase the size of the saturated absorption dips. Optical pumping due to the probe beam can also affect saturated absorption measurements, particularly if the probe laser intensity is high. In this case, the probe beam shelves the atoms involved in the absorption at all frequencies, not just at the saturated absorption dips.

Surprisingly, optical pumping does not significantly change the predicted form for the absorption signals. Largely, its effect is to change the widths $(\Gamma's)$, the saturation intensities (I_{sat} 's) and the strengths (κ 's) appearing in the formulae.

One common application of saturated absorption spectroscopy is in measuring the hyperfine splittings of atomic spectral lines. They are so small that Doppler broadening normally makes it impossible to resolve them. will use saturated absorption spectroscopy to study the hyperfine splittings in the rubidium atom and thus will need to know a little about its energy level structure.

In principle, quantum mechanical calculations can accurately predict the energy levels and electronic wavefunctions of multielectron atoms. In practice, the calculations are difficult and this section will only present enough of the results to appreciate the basic structure of rubidium's energy levels. You should consult the references for a more in-depth treatment of the topic.

The crudest treatment of the energy levels in multielectron atoms is called the central field approximation (CFA). In this approximation the nuclear and electron magnetic moments are ignored and the atomic electrons are assumed to interact, not with each other, but with an effective radial electric field arising from the average charge distribution from the nucleus and all the other electrons in the

Solving for the energy levels in the CFA leads to an atomic configuration in which each electron is described by the following quantum numbers:

- 1. The principal quantum number n (allowed integer values greater than zero) characterizes the radial dependence of the wavefunction.
- 2. The orbital angular momentum quantum number ℓ (allowed values from 0 to n-11) characterizes the angular dependence of the wavefunction and the magnitude

of the orbital angular momentum ℓ of an Fine structure levels individual electron.³

- 3. The magnetic quantum number m_{ℓ} (allowed values from $-\ell$ to ℓ) further characterizes the angular dependence of the wavefunction and the projection of ℓ on a chosen quantization axis.⁴
- 4. The electron spin quantum number s (only allowed value equal to 1/2) characterizes the magnitude of the intrinsic or spin angular momentum s of an individual electron.
- 5. The spin projection quantum number m_s (allowed values $\pm 1/2$) characterizes the projection of s on a chosen quantization axis.

The rubidium atom (Rb) has atomic number 37. In its lowest (ground state) configuration it has one electron outside an inert gas (argon) core and is described with the notation $1s^22s^22p^63s^23p^63d^{10}4s^24p^65s$. The integers 1 through 5 above specify principal quantum numbers n. The letters s, p, and d specify orbital angular momentum quantum numbers ℓ as 0, 1, and 2, respectively. The superscripts indicate the number of electrons with those values of n and ℓ .

The Rb ground state configuration is said to have filled shells to the 4p orbitals and a single valence (or optical) electron in a 5s orbital. The next higher energy configuration has the 5s valence electron promoted to a 5p orbital with no change to the description of the remaining 36 electrons.

Within a configuration, there can be several fine structure energy levels differing in the energy associated with the coulomb and spinorbit interactions. The coulomb interaction is associated with the normal electrostatic potential energy kq_1q_2/r_{12} between each pair of electrons and between each electron and the nucleus. (Most, but not all of the coulomb interaction energy is included in the configuration energy.) The spin-orbit interaction is associated with the orientation energy $-\mu \cdot \mathbf{B}$ of the magnetic dipole moment μ of each electron in the internal magnetic field **B** of the atom. The form and strength of these two interactions in rubidium are such that the energy levels are most accurately described in the L-S or Russell-Saunders coupling scheme. L-S coupling introduces new angular momentum quantum numbers L, S, and J as described next.

1. L is the quantum number describing the magnitude of the total orbital angular momentum L, which is the sum of the orbital angular momentum of each electron:

$$\mathbf{L} = \sum \boldsymbol{\ell}_i \tag{33}$$

2. S is the quantum number describing the magnitude of the total electronic spin angular momentum S, which is the sum of the spin angular momentum of each electron:

$$\mathbf{S} = \sum \mathbf{s}_i \tag{34}$$

3. J is the quantum number describing the magnitude of the total electronic angular momentum J, which is the sum of the total orbital and total spin angular momentum:

$$\mathbf{J} = \mathbf{L} + \mathbf{S} \tag{35}$$

³Angular momentum operators such as ℓ satisfy an eigenvalue equation of the form $\ell^2 \psi = \ell(\ell+1)\hbar^2 \psi$.

⁴Angular momentum projection operators such as ℓ_z satisfy an eigenvalue equation of the form $\ell_z \psi =$ $m_{\ell}\hbar\psi$.

The values for L and S and J are specified in a notation $^{(2S+1)}L_J$ invented by early spectroscopists. The letters S, P, and D (as with the letters s, p, and d for individual electrons) are used for L and correspond to L=0, 1, and 2, respectively. The value of (2S+1) is called the *multiplicity* and is thus 1 for S=0 and called a singlet, 2 for S=1/2 (doublet), 3 for S=1 (triplet), etc. The value of J (with allowed values from |L-S| to L+S) is annotated as a subscript to the value of L.

The sum of ℓ_i or \mathbf{s}_i over all electrons in any filled orbital is always zero. Thus for Rb configurations with only one valence electron, there is only one allowed value for L and S: just the value of ℓ_i and s_i for that electron. In its ground state (5s) configuration, Rb is described by L=0 and S=1/2. The only possible value for J is then 1/2 and the fine structure state would be labeled ${}^2S_{1/2}$. Its next higher (5p) configuration is described by L=1 and S=1/2. In this configuration there are two allowed values of J: 1/2 and 3/2 and these two fine structure states are labeled ${}^2P_{1/2}$ and ${}^2P_{3/2}$.

Hyperfine levels

Within each fine structure level there can be an even finer set of *hyperfine* levels differing in the orientation energy (again, a $-\mu \cdot \mathbf{B}$ type energy) associated with the nuclear magnetic moment in the magnetic field of the atom. The nuclear magnetic moment is much smaller

than the electron magnetic moment and this is why the hyperfine splittings are so small. The nuclear magnetic moment is proportional to the spin angular momentum \mathbf{I} of the nucleus, whose magnitude is described by the quantum number I. Allowed values for I depend on nuclear structure and vary with the isotope.

The hyperfine energy levels depend on the the total angular momentum \mathbf{F} of the atom: the sum of the total electron angular momentum \mathbf{J} and the nuclear spin angular momentum \mathbf{I} :

$$\mathbf{F} = \mathbf{J} + \mathbf{I} \tag{36}$$

The magnitude of \mathbf{F} is characterized by the quantum number F with allowed values from |J-I| to J+I. Each state with a different value of F will have a slightly different energy due to the interaction of the nuclear magnetic moment and the internal field of the atom. There is no special notation for the labeling of hyperfine states and F is usually labeled explicitly in energy level diagrams.

There are two naturally occurring isotopes of Rb: 72% abundant ⁸⁷Rb with I = 3/2 and 28% abundant ⁸⁵Rb with I = 5/2. For both isotopes, this leads to two hyperfine levels within the ²S_{1/2} and ²P_{1/2} fine structure levels (F = I - 1/2 and F = I + 1/2) and four hyperfine levels within the ²P_{3/2} fine structure level (F = I - 3/2, I - 1/2, I + 1/2, I + 3/2).

The energies of the hyperfine levels can be expressed (relative to a "mean" energy E_J for the fine structure state) in terms of two hyperfine constants A and B by the Casimir formula

$$E_{F} = E_{J} + A \frac{\kappa}{2}$$

$$+ B \frac{3\kappa(\kappa+1)/4 - I(I+1)J(J+1)}{2I(2I-1)J(2J-1)}$$
(37)

where $\kappa = F(F+1) - J(J+1) - I(I+1)$. (If either I = 1/2 or J = 1/2, the term containing B must be omitted.)

 $^{^5 {\}rm The}$ terms singlet, doublet, triplet etc. are associated with the number of allowed values of J typically possible with a given L and S (if $L \geq S$). Historically, the terms arose from the number of closely-spaced spectral lines typically (but not always) observed in the decay of these levels. For example, the sodium doublet at 589.0 and 589.6 nm occurs in the decay of the $^2{\rm P}_{1/2}$ and $^2{\rm P}_{3/2}$ fine structure levels to the $^2{\rm S}_{1/2}$ ground state. While the $^2{\rm P}_{1/2}$ and $^2{\rm P}_{3/2}$ are truly a doublet of closely-spaced energy levels, the $^2{\rm S}_{1/2}$ state has only one allowed value of J.

Iso	fss	A	В
85 Rb	$^{2}S_{1/2}$	1011.91	
	${}^{2}\mathrm{P}_{1/2}$	120.72	
	${}^{2}\mathrm{P}_{3/2}$	25.01	25.88
$^{87}\mathrm{Rb}$	$^{2}S_{1/2}$	3417.34	
	${}^{2}\mathrm{P}_{1/2}$	406.20	
	${}^{2}\mathrm{P}_{3/2}$	84.80	12.52

Table 1: Hyperfine constants A and B (in MHz) for the lowest three fine structure states in the two naturally-occurring Rb isotopes

Figure 10 shows the configuration-fine structure-hyperfine energy structure of the Rb atom. The scaling is grossly inaccurate. The energy difference between the 5s and 5p configurations is around 1.6 eV, the difference between the $^2P_{1/2}$ and $^2P_{3/2}$ fine structure levels is around 0.03 eV, and the differences between

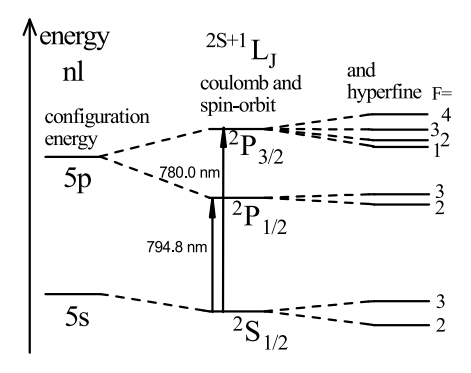


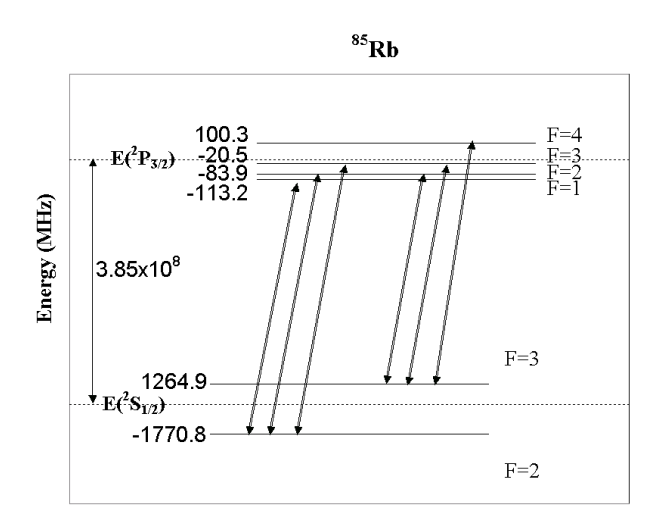
Figure 10: Energy structure of the lowest levels in 85 Rb, (I=5/2). Energy increases toward the top, but the levels are not shown to scale; the separation between the 5s and 5p configuration energies is about 50 times bigger than the spacing between the 2 P_{1/2} and 2 P_{3/2} fine structure levels, and it is about 10^5 times bigger than the spacing within any group of hyperfine levels.

hyperfine levels are less than 0.00003 eV.

Transitions

The ${}^2S_{1/2}$ to ${}^2P_{1/2}$ transitions are all around 795 nm while the ${}^2S_{1/2}$ to ${}^2P_{3/2}$ transitions are all around 780 nm. We will only discuss the 780 nm transitions that can be reached with the laser used in this experiment. Dipole transitions follow the selection rule $\Delta F = 0, \pm 1$. Thus, in each isotope, the allowed transitions from the $^2\mathrm{S}_{1/2}$ to $^2\mathrm{P}_{3/2}$ fall into two groups of three, with each group labeled by the F of the ²S_{1/2} state. Because the hyperfine splitting between the two ${}^{2}S_{1/2}$ levels is large compared to the hyperfine splittings among the four ²P_{3/2} levels, the groups will be well separated from each other. Within each group, the three possible transitions can be labeled by the F' of the ${}^{2}P_{3/2}$ state. These three transitions will be more closely spaced in energy.

C.Q. 3 The energy level diagrams of Fig. 11 are based on the information in Table 1 with Eq. 37. Use the same information to create a table and scaled stick spectrum for all twenty-four 780 nm resonances (including the crossover resonances) occurring in both isotopes. The horizontal axis should be at least 25 cm long and labeled in MHz. For the figure, draw a one- or two-centimeter vertical line along the horizontal frequency axis at the position of each resonance. Label the isotopes and the F of the ${}^2S_{1/2}$ level for each of the four groups and within each group label the value of F' in the ${}^{2}P_{3/2}$ level for each of the three normal resonances and the two values of F' for each of the three crossover resonances. Also label their transition energies (in MHz) relative to the overall 385 THz average transition frequency. Hint: you should get the lowest two resonances in ⁸⁷Rb — a normal resonance between the F = 2 and F' = 1 levels 2793.1



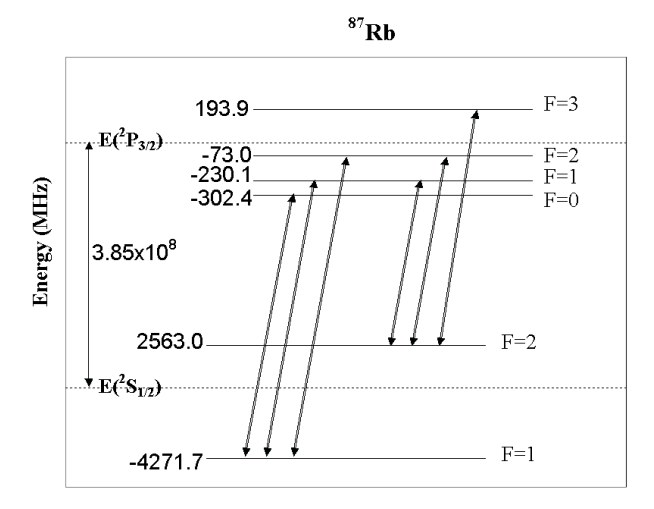


Figure 11: Energy levels for 85 Rb and 87 Rb (not to scale). Note that the hyperfine splittings are about an order of magnitude larger in the ground 2 S_{1/2} levels compared to the excited 2 P_{3/2} levels.

MHz below the average and a crossover resonance between the F=2 and F'=1,2 levels 2714.5 MHz below the average. The highest energy resonance is again in ^{87}Rb ; a normal resonance from F=1 to F'=2 4198.7 MHz above the average.

Apparatus

Laser Safety

The diode laser used in this experiment has sufficient intensity to permanently damage your eye. In addition, its wavelength (around 780 nm) is nearly invisible. Safety goggles must be worn when working on this experiment. You should also follow standard laser safety procedures as well.

- 1. Remove all reflective objects from your person (e.g., watches, shiny jewelry).
- 2. Make sure that you block all stray reflections coming from your experiment.
- 3. Never be at eye level with the laser beam (e.g., by leaning down).

4. Take care when changing optics in your experiment so as not to inadvertently place a highly reflective object (glass, mirror, post) into the beam.

The layout of the saturated absorption spectrometer is shown in Fig. 12. Two weak beams are reflected off the front and rear surfaces of a thick beam splitter (about 4% each). One (the probe beam) is directed through the rubidium cell from left to right and then onto a photodiode detector. The other is directed through a Fabry-Perot interferometer and onto a second photodiode detector for calibrating the frequency scan.

The strong beam is transmitted through the thick beam splitter. The two lenses after the beam splitter should be left out at first and only used if needed to expand the laser beam. This is the pump beam passing through the cell from right to left, overlapping the probe beam and propagating in the opposite direction. (The intersection angle is exaggerated in the figure.)

You should not adjust the components from the thick beam splitter back to the laser.

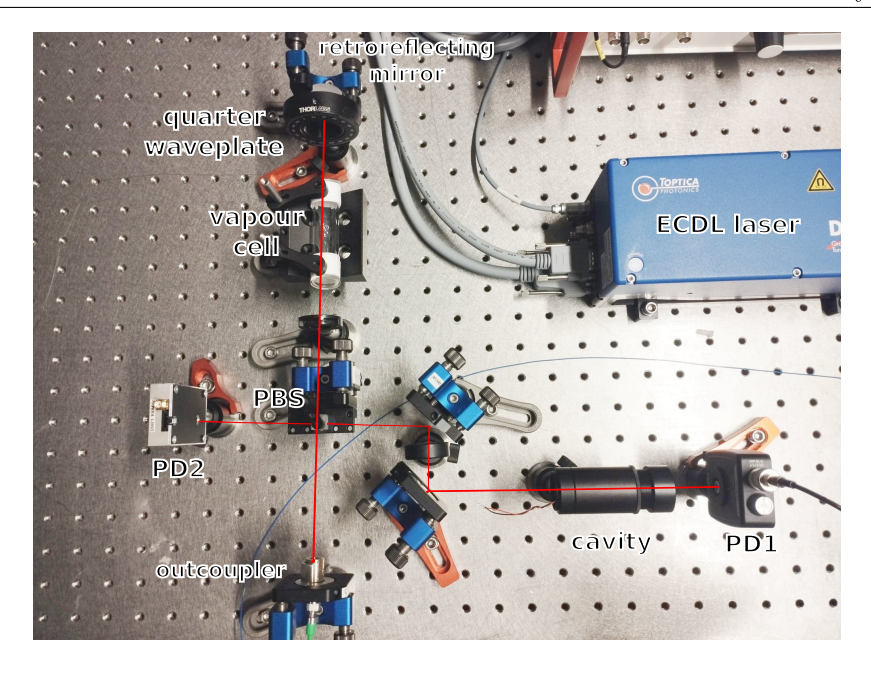


Figure 12: Experimental setup. Light from the laser is outcoupled and sent onto beam splitter. Beam reflected on a PBS (polarizing beam splitter) is sent to the optical cavity, the light passing through the cavity acts as a pump beam. After vapour cell, the pump beam passes through a quarter waveplate and is reflected back with a mirror. Reflected beam is weaker and acts as a probe beam. Pump and probe are overlaped with each other. The probe beam is sent onto a photodiode to observe the spectrum.

The diode laser

A schematic of our diode laser is shown in Fig. 13. The American Journal of Physics article on which its construction is based as well as manufacturer literature on the laser diode used in the laser can be found in the auxiliary material.

The frequency of the laser depends on three parameters:

- The laser temperature
- The laser current
- The position and orientation of the grating

The laser temperature and current set the frequency range over which the diode laser will operate (coarse tuning). Within this range, the laser frequency can be continuously scanned using the position and orientation of the grating (fine tuning). Fine tuning of the laser frequency is accomplished by a piezoelectric transducer (PZT) located in the grating mount. The PZT expands in response to a

voltage (0-150 V) from the PZT controller (described later). The voltage can be adjusted manually or under computer-control.

As the laser cavity length varies, because the number of waves in the cavity will stay constant (for a while), the wavelength and therefore the laser frequency will vary as well. But if the cavity length change goes too far, the number of half-wavelengths inside the cavity will jump up or down (by one or two) so that the laser frequency will jump back into the range set by the temperature and current. These jumps are called $mode\ hops$. Continuous frequency tuning over the four hyperfine groups ($\approx 8\,\mathrm{GHz}$) without a mode hop can only be achieved if the settings for the temperature and current are carefully optimized.

The beam profile (intensity pattern in a cross-section of the laser beam) from the laser head is approximately a 1.5×3 mm elliptical spot. An anamorphic prism pair is used to transform this to a circular pattern. In addition, lenses may be used to change the beam diameter.

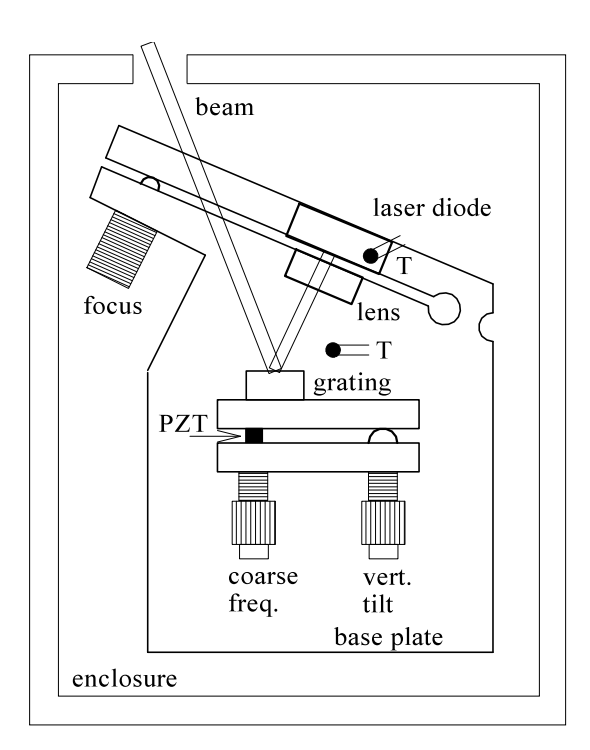


Figure 13: Schematic of our diode laser. Except for the thermistors (T), the temperature control elements and electrical connections are not shown.

Beam Paths

Several beams are created from the single beam coming from the laser. The polarizing beam splitter and the quarter-wave plate help prevent the pump beam from feeding back into the laser cavity thereby affecting the laser output.

The thick beam splitter creates the three beams used in the experiment.

Two beams create the probe beam and the beam sent through the Fabry-Perot interferometer. Each of these beams contains about 4% of the laser output. About 92% passes through this beam splitter to become the pump beam.

You should also check for additional beams,

particularly from the polarizing and nonpolarizing beam splitters, and use beam blocks for any that are directed toward areas where people have access.

Photodetectors

Two photodetectors are used to monitor the laser beam intensities. A bias voltage from a battery ($\approx 10 \, \mathrm{V}$) is applied to the photodetector which then acts as a current source. The current is proportional to the laser power impinging on the detector and is converted to a voltage (for measurement) either by sending it through a low noise current amplifier or by letting it flow through a resistor to ground. With the latter method, the voltage developed across the resistor subtracts from the battery voltage and the resistance should be adjusted to keep it below one volt.

Fabry-Perot Interferometer

Once the laser temperature has stabilized and a laser current has been set, a voltage ramp will be applied to the PZT causing the laser frequency to smoothly sweep over several resonance frequencies of the rubidium atoms in the cell. The laser frequency during the sweep is monitored using a confocal Fabry-Perot interferometer. The Fabry-Perot consists of two partially transmitting mirrors - one planar and one convex with radius of curvature R=100 mm as shown in Fig. 14.

With the laser well aligned going into the Fabry-Perot cavity, Fig. 15 shows how much is transmitted through the cavity as a function of the laser frequency. The Fabry-Perot only transmits the laser beam at a set of discrete frequencies separated by the free spectral range (FSR). For a plano-convex Fabry-Perot it is given by:

$$FSR = \frac{c}{4L} \tag{38}$$

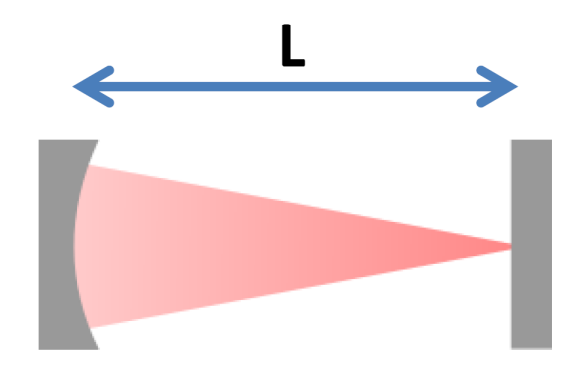


Figure 14: The optical resonator or Fabry-Perot interferometer consists of two partially transmitting mirrors facing each other.

where L is the distance between the mirrors. Consequently, as the frequency of the laser beam going into the cavity is swept, the transmission (as monitored by a photodetector on the other side of the cavity) will show a series of peaks separated by the FSR. These peaks (or fringes) will be monitored simultaneously with absorption through the rubidium and will serve as frequency markers for how the laser frequency is changing during the sweep.

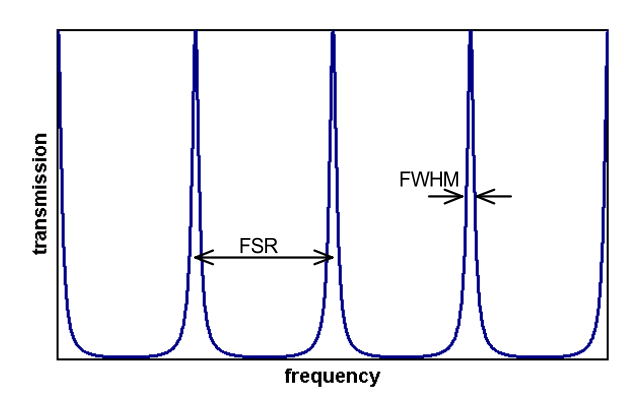


Figure 15: The transmitted intensity for a well aligned Fabry-Perot interferometer shows sharp peaks equally spaced in frequency.

Rb vapor cell

The Rb vapor cell is a glass cell filled with natural rubidium having two isotopes: 85 Rb and 87 Rb. The vapor pressure of rubidium inside the cell is determined by the cell temperature and is about 4×10^{-5} Pa at room temperature.

Low-noise current amplifier

The low noise current amplifier can be used to amplify and filter the photodetector signal. This signal will change at a rate which depends on the rate at which you scan the laser frequency. For a very slow scan, the interesting parts of the signal will change very slowly and you can use the low pass filter function of the amplifier to reduce the higher frequency noise like 60Hz pick-up. The low pass filter should not change your signal if the cutoff frequency is set properly. Another possibility is to scan rather fast and use the bandpass filter function to reduce the low and high frequency noise. You should play with these options a bit and try to find the optimum setting for your scan rate and detector noise.

Alignment procedure

Most students have difficulties aligning the position and propagation direction of a laser beam simultaneously—usually due to a mixture of inexperience and impatience. In the following we describe the standard alignment procedure. As usual, standard procedures are not applicable to all cases but they should give you an idea how do do it.

Task: Align a laser beam to propagate along a particular axis in the apparatus, e.g., the axis of our Fabry-Perot resonator. This alignment procedure is called beam walking and requires two mirrors in adjustable mirror mounts.

• Coarse alignment:

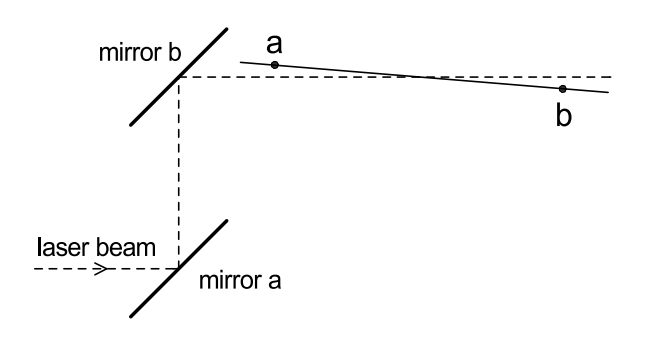


Figure 16: Procedure to align the laser beam (dashed line) along a prescribed line (solid line ab). Pick two reference points a and b and use the first mirror to align the laser to point a and the second mirror to align the laser to point b. Iterate until laser beam is perfectly aligned.

- 1. Pick two reference points along the target axis. These points should be reasonably far apart from each other.
- 2. Use the first alignment mirror to align the laser on the first reference point.
- 3. Use the second alignment mirror to align the laser on the second reference point.
- 4. Iterate points 2 and 3 until the laser beam is aligned as well as possible with respect to the optical axis. You might overshoot in step 2 or step 3 occasionally to accelerate the procedure.
- Fine alignment or optimizing the signal:
 - 1. Display the signal you wish to optimize. For example, the photodetector signal after the Fabry-Perot resonator.

- 2. Optimize the signal with the first mirror in the horizontal and vertical directions.
- 3. Optimize the signal with the second mirror in the horizontal and vertical directions.
- 4. Use the first mirror to de-optimize the signal very slightly in the horizontal direction. Remember the direction you moved the mirror.
- 5. Use the second mirror to re-optimize the signal again.
- 6. Compare this signal with the signal you had before step 4. If the signal improved repeat step 4 moving in the same direction. If the signal got worse, repeat step 4 moving in the opposite direction.
- 7. Iterate until you can't further improve the signal.
- 8. Do the same for the vertical direction until you can't improve the signal anymore.
- 9. Iterate steps 4 to 8 until you can't improve the signal furthermore.

This procedure requires some patience and can not be done in five minutes.

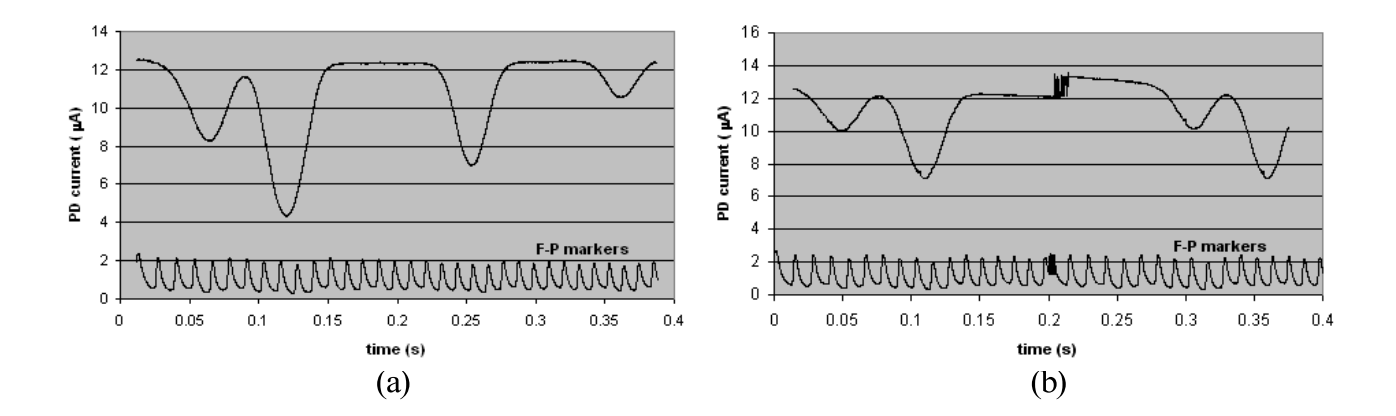


Figure 17: Single-beam Rb absorption spectra. (a) Shows a laser frequency sweep of about 8 GHz without a mode hop over the appropriate region of interest for the Rb hyperfine levels near 780 nm. (b) Shows a sweep with a mode hop around 0.2 s.

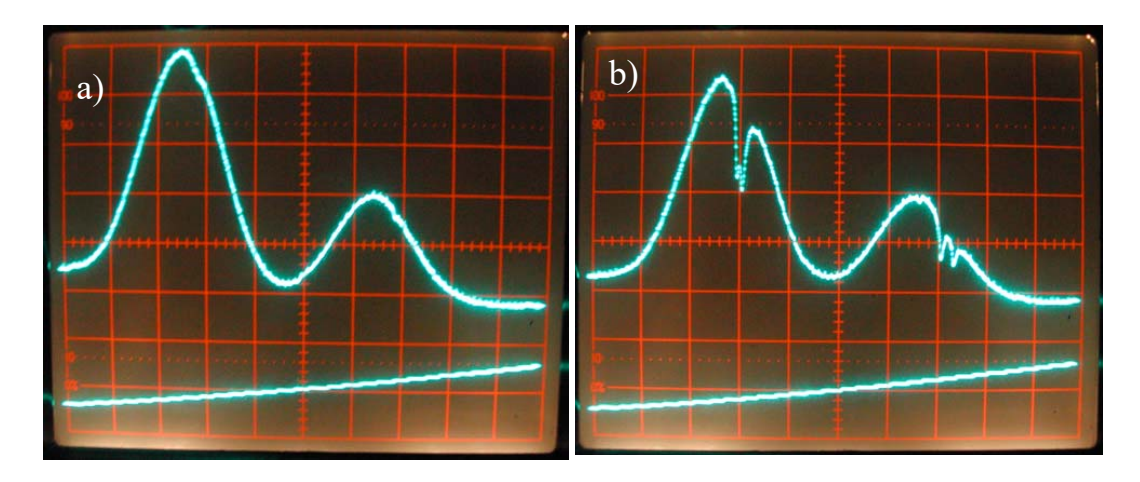


Figure 18: Comparison of a) absorption spectrum with one beam only, b) saturated absorption spectroscopy of rubidium vapour.

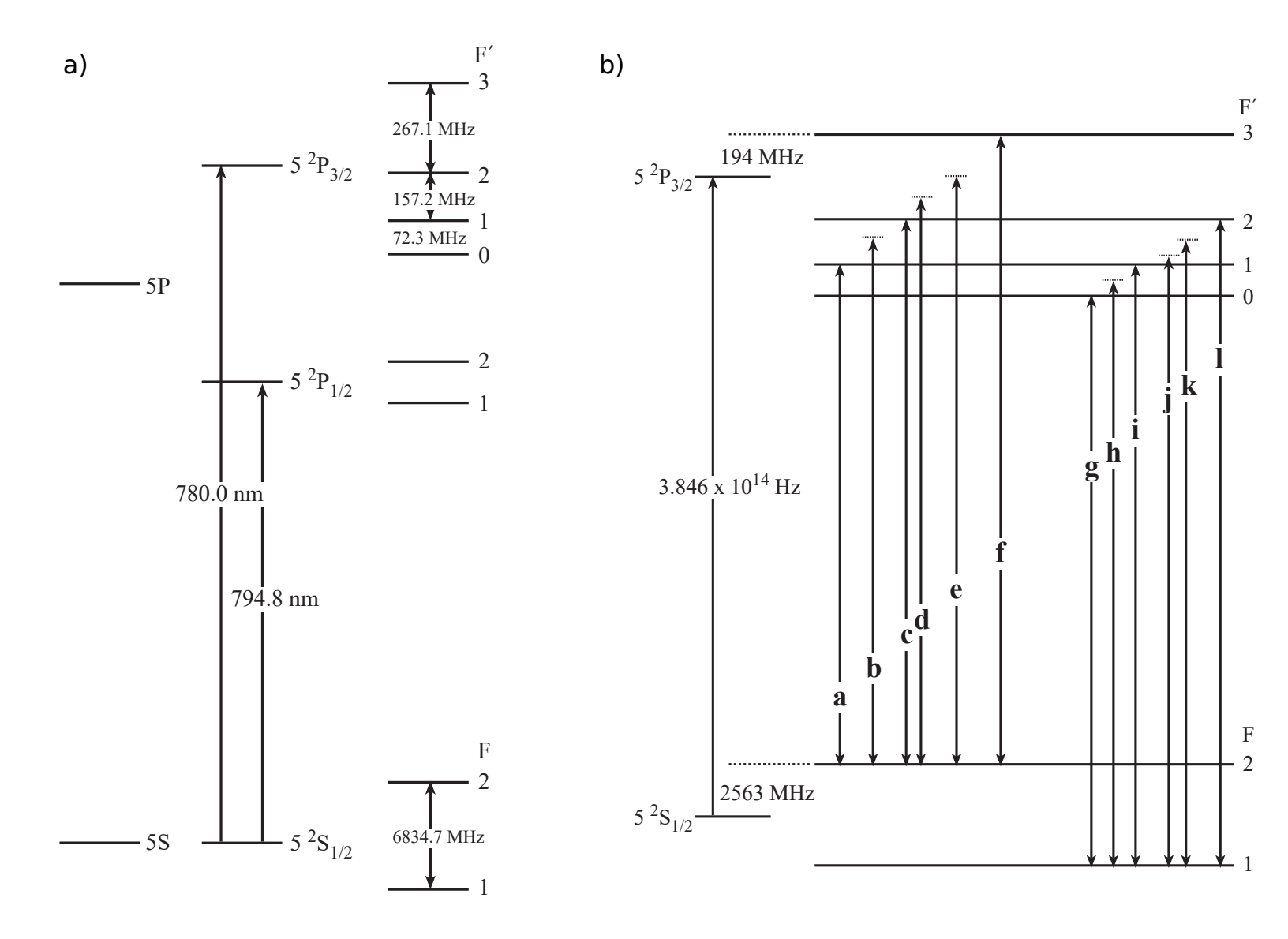


Figure 19: a) Fine and hyperfine energy levels of ⁸⁷Rb, b) transitions that can be observed when saturation absorption spectroscopy is performed. Dotted lines indicate crossover resonances.